INTERNATIONAL JOURNAL OF ADAPTIVE CONTROL AND SIGNAL PROCESSING
Int. J. Adapt. Control Signal Process. 2008; **22**:968–986
Published online 17 October 2008 in Wiley InterScience (www.interscience.wiley.com). DOI: 10.1002/acs.1062

A fractional adaptation law for sliding mode control

Mehmet Önder Efe*, † and Coşku Kasnakoğlu

Department of Electrical and Electronics Engineering, TOBB Economics and Technology University, Sögütözü Cad. No. 43, TR-06560 Sögütözü, Ankara, Turkey

SUMMARY

This paper presents a novel parameter tuning law that forces the emergence of a sliding motion in the behavior of a multi-input multi-output nonlinear dynamic system. Adaptive linear elements are used as controllers. Standard approach to parameter adjustment employs integer order derivative or integration operators. In this paper, the use of fractional differentiation or integration operators for the performance improvement of adaptive sliding mode control systems is presented. Hitting in finite time is proved and the associated conditions with numerical justifications are given. The proposed technique has been assessed through a set of simulations considering the dynamic model of a two degrees of freedom direct drive robot. It is seen that the control system with the proposed adaptation scheme provides (i) better tracking performance, (ii) suppression of undesired drifts in parameter evolution, (iii) a very high degree of robustness and improved insensitivity to disturbances and (iv) removal of the controller initialization problem. Copyright © 2008 John Wiley & Sons, Ltd.

Received 6 December 2007; Revised 25 June 2008; Accepted 4 July 2008

KEY WORDS: fractional tuning laws; adaptive sliding mode control; adaptation; fractional order control

1. INTRODUCTION

Owing to the linearity between its inputs and the output, and the simplicity brought about by this fact, adaptive linear element (ADALINE) structure has been used in many applications of systems and control engineering presumably under different names. From this perspective, proportional integral derivative (PID) controllers, state feedback controllers and finite impulse response filters are just to name a few of ADALINE applications. The output of an ADALINE is a weighted sum of its inputs and the weight associated to each input is adjustable. As discussed in detail by Haykin [1] and Jang *et al.* [2], ADALINEs are the building blocks of neural networks and some

*Correspondence to: Mehmet Önder Efe, Department of Electrical and Electronics Engineering, TOBB Economics and Technology University, Sögütözü Cad. No. 43, TR-06560 Sögütözü, Ankara, Turkey.
†E-mail: onderefe@etu.edu.tr

Contract/grant sponsor: Turkish Scientific Council (TÜBİTAK); contract/grant number: 107E137

types of fuzzy systems. The driving force for devising such complicated architectures was the fact that ADALINEs were so simple that they could not capture complex input output relations with frozen parameters. Yet it was possible to implement the ADALINE as an adaptive system, which can respond appropriately by an adaptation scheme. Given a task to be accomplished, the process describing the best evolution of the adjustable parameters is the process of learning, which is sometimes called adaptation, tuning, adjustment or optimization, all referring to the same reality in the context of adaptive systems. Many approaches have been proposed, perceptron learning rule, gradient descent, Levenberg–Marquardt technique, Lyapunov-based techniques are just to name a few; a good treatment can be found in [2]. A common feature of all these methods is the fact that the differentiation and integration, or shortly differintegration, of quantities are performed in integer order, i.e. $\mathbf{D} := \mathrm{d}/\mathrm{d}t$ for the differentiation with respect to t and $\mathbf{I} = \mathbf{D}^{-1}$ for integration over t in the usual sense. A significantly different branch of mathematics, called fractional calculus, suggests operators $\mathbf{D}^{\beta}$ with $\beta \in \Re$ [3, 4] and it becomes possible to write $\mathbf{D} f = \mathbf{D}^{1/2}(\mathbf{D}^{1/2} f)$. Expectedly, Laplace and Fourier transforms in fractional calculus are available to exploit in closed loop control system design, involved with s^{β} or $(\mathrm{j}\omega)^{\beta}$ generic terms, respectively.

Fractional calculus and dynamics described by fractional differential equations (FDEs) are becoming more and more popular as the underlying facts about the differentiation and integration is significantly different from the integer order counterparts and, beyond this, many real life systems are described better by FDEs, e.g. heat equation, telegraph equation and a lossy electric transmission line are all involved with fractional order differintegration operators. A majority of works published so far has concentrated on the fractional variants of the PID controller, which has fractional order differentiation and fractional order integration, implemented for the control of linear dynamic systems, for which the issues of parameter selection, tuning, stability and performance are rather mature concepts utilizing the results from complex analysis and frequency domain methods of control theory (see [5]) than those involving the nonlinear models (see [6]) and parameter changes in the approaches.

Parameter tuning in adaptive control systems is a central part of the overall mechanism alleviating the difficulties associated with the changes in the parameters that influence the closed loop performance. Many remarkable studies are reported in the past and the field of adaptation has become a blend of techniques of dynamical systems theory, optimization, heuristics (intelligence) and soft computing. Today, the advent of very high-speed computers and networked computing facilities, even within microprocessor-based systems, tuning of system parameters based upon some set of observations and decisions has greatly been facilitated. In [7], an in-depth discussion for parameter tuning in continuous and discrete time is presented. Particularly, for gradient descent rule for model reference adaptive control, which is considered in the integer order in [7], has been implemented in fractional order by Vinagre *et al.* [8], where the integer order integration is replaced with an integration of fractional order 1.25, and by Ladaci and Charef [9], where the good performance in noise rejection is emphasized. In [10], dynamic model of a ground vehicle is given and an adaptive control law based on the gain adjustment is derived, the adaptation law is changed to a fractional order and the benefits of using this form are shown through simulations.

Regarding the sliding mode control, Calderón *et al.* [11] describes the switching function by a fractional order PID controller and variants of it. The analysis continues with the computation of the first derivative of the switching function and relevant reaching conditions are derived. The method is experimented on a buck converter. In [12], sliding mode control framework is studied. A double integrator and the conditions of stability are described. Modification of the equivalent control is performed so that a fractionally integrated sign term provides reduction in high-frequency

DOI: 10.1002/acs

switching. In both papers, the stability has been analyzed through checking whether $s\dot{s}<0$ is satisfied, with s being the switching function.

The purpose of this paper is to present an adaptation approach that yields (i) better robustness and noise rejection capabilities than those utilizing traditional integer order operators, (ii) nondrifting parametric evolution when the essential factor driving the adaptation scheme is noise, (iii) better tracking capability and better system response and (iv) removal of the controller initialization problem. The four features mentioned above constitute the major results and contributions of the paper.

This paper is organized as follows: In the following section, we give the Riemann–Liouville definitions of fractional operators used throughout the paper. The sliding mode control in the traditional sense is summarized in the third section. In the fourth section, a fractional order adaptation scheme is introduced and the stability analysis with conditions for hitting in finite time is discussed. In this section, the parameter adjustment for the ADALINE is viewed as a supervised adaptation scheme. In the fifth section, the conditions for applying the scheme as an unsupervised technique are presented. The dynamical description of a two degrees of freedom (DOF) SCARA[‡]-type direct drive robot is presented in the sixth section. Simulation results and the concluding remarks constitute the last part of the paper.

2. FRACTIONAL ORDER DERIVATIVE AND INTEGRAL

Given $0<\beta<1$, Riemann–Liouville definition of the βth order fractional derivative operator ${}_0\mathbf{D}_t^{\beta}$ is given by

$$\begin{aligned} f^{(\beta)}(t) &= {}_0\mathbf{D}_t^{\beta} f(t) \\ &= \frac{1}{\Gamma(1-\beta)} \frac{\mathrm{d}}{\mathrm{d}t} \int_0^t (t-\xi)^{-\beta} f(\xi)\, \mathrm{d}\xi \end{aligned} \tag{1}$$

where $\Gamma(\cdot)$ is the gamma function[§] generalizing the factorial for noninteger arguments. According to this definition, the derivative of a time function $f(t)=t^{\alpha}$ with $\alpha>-1, t\geqslant 0$ is evaluated as

$${}_0\mathbf{D}_t^{\beta} t^{\alpha} = \frac{\Gamma(\alpha+1)}{\Gamma(\alpha+1-\beta)} t^{\alpha-\beta} \tag{2}$$

Likewise, Riemann–Liouville definition of the βth order fractional integration operator ${}_0\mathbf{I}_t^{\beta}$ is given by

$${}_0\mathbf{I}_t^{\beta} f(t) = \frac{1}{\Gamma(\beta)} \int_0^t (t-\xi)^{\beta-1} f(\xi)\, \mathrm{d}\xi \tag{3}$$

In addition to these definitions, following equalities are helpful in understanding the presented approach. For $0<\beta<1$ and a finite end time, say t_h, the integral of the derivative is evaluated as

[‡]Selectively compliant articulated robot arm.

[§]The gamma function is defined as $\Gamma(\beta)=\int_0^{\infty} \mathrm{e}^{-t} t^{\beta-1}\, \mathrm{d}t$.

DOI: 10.1002/acs

given in the following equation [4]:

$$ {}_0\mathbf{I}_{t_h}^{\beta} f^{(\beta)} = f(t_h) - f^{(\beta-1)}(0)\frac{t_h^{\beta-1}}{\Gamma(\beta)} \tag{4} $$

The integral of a constant, say, $\mathscr{B}$ with the same integration limits is given as in the following equation:

$$ {}_0\mathbf{I}_{t_h}^{\beta} \mathscr{B} = \frac{t_h^{\beta}}{\Gamma(1+\beta)}\mathscr{B} \tag{5} $$

The material presented in the sequel is based on the above definitions of fractional differentiation and integration.

3. AN OVERVIEW OF SLIDING MODE CONTROL

Owing to the robustness against uncertainties and disturbances, and the invariance properties during the sliding regime, sliding mode control has become a popular design approach that was implemented successfully for the control of robots [13, 14].

Consider a general dynamic system described by

$$ \theta_i^{(r_i)} = f_i(\mathbf{\Theta}) + \tilde{f}_i(\mathbf{\Theta}) + \sum_{j=1}^{m} (g_{ij}(\mathbf{\Theta}) + \tilde{g}_{ij}(\mathbf{\Theta}))\tau_j, \quad i = 1, 2, \ldots, n \tag{6} $$

where $\mathbf{\Theta} = (\theta_1, \dot{\theta}_1, \ldots, \theta_1^{(r_1-1)}, \theta_2, \dot{\theta}_2, \ldots, \theta_2^{(r_2-1)}, \ldots, \theta_n, \dot{\theta}_n, \ldots, \theta_n^{(r_n-1)})^{\mathrm{T}}$ is the state vector of the entire system, r_i is the order of the ith subsystem, $f_i(\mathbf{\Theta})$ and $g_{ij}(\mathbf{\Theta})$ are scalar functions of the state vector describing the nominal (known) part of the dynamics, $\tilde{f}_i(\mathbf{\Theta})$ and $\tilde{g}_{ij}(\mathbf{\Theta})$ are the bounded uncertainties on these functions and the input vector $\mathbf{T} = (\tau_1, \tau_2, \ldots, \tau_n)^{\mathrm{T}}$ is the manipulated variable. This system of equations can be rewritten compactly as

$$ \dot{\mathbf{\Theta}} = F(\mathbf{\Theta}) + \tilde{F}(\mathbf{\Theta}) + (G(\mathbf{\Theta}) + \tilde{G}(\mathbf{\Theta}))\mathbf{T} \tag{7} $$

where $F(\mathbf{\Theta})$ and $\tilde{F}(\mathbf{\Theta})$ are $\sum_{i=1}^{n} r_i \times 1$ dimensional vectors and $G(\mathbf{\Theta})$ and $\tilde{G}(\mathbf{\Theta})$ are $\sum_{i=1}^{n} r_i \times n$ dimensional matrices. The designer has the nominal plant dynamics given by $\dot{\mathbf{\Theta}} = F(\mathbf{\Theta}) + G(\mathbf{\Theta})\mathbf{T}$.

Standard approach for the design of a sliding mode controller entails a switching function defined as

$$ \begin{aligned} \mathbf{s} &= (s_1, s_2, \ldots, s_n)^{\mathrm{T}} \\ &= \mathbf{\Lambda}(\mathbf{\Theta} - \mathbf{\Theta}_d) \end{aligned} \tag{8} $$

where $\mathbf{\Theta}_d = (\theta_{d,1}, \dot{\theta}_{d,1}, \ldots, \theta_{d,1}^{(r_1-1)}, \theta_{d,2}, \dot{\theta}_{d,2}, \ldots, \theta_{d,2}^{(r_2-1)}, \ldots, \theta_{d,n}, \dot{\theta}_{d,n}, \ldots, \theta_{d,n}^{(r_n-1)})^{\mathrm{T}}$ is the vector of desired states and the locus described by $\mathbf{s} = \mathbf{0}$ corresponds to the sliding manifold or the switching hypersurface. The entries of $\mathbf{\Lambda}$ are chosen such that the ith component of the switching manifold has the structure

$$ s_i = \left(\frac{\mathrm{d}}{\mathrm{d}t} + \lambda_i\right)^{r_i - 1} (\theta_i - \theta_{d,i}), \quad i = 1, 2, \ldots, n \tag{9} $$

DOI: 10.1002/acs

where $\lambda_i > 0$. Choosing a Lyapunov function candidate as in (10) and setting the control vector as given in (11), one gets the equality in (12) provided that the inverse $(\mathbf{\Lambda} G(\mathbf{\Theta}))^{-1}$ exists:

$$V = \tfrac{1}{2}\mathbf{s}^{\mathrm{T}}\mathbf{s} \tag{10}$$

$$\boldsymbol{\tau}_{\mathbf{SMC}} = -(\mathbf{\Lambda} G(\mathbf{\Theta}))^{-1}\mathbf{\Lambda}(F(\mathbf{\Theta}) - \dot{\mathbf{\Theta}}_d) - (\mathbf{\Lambda} G(\mathbf{\Theta}))^{-1}\mathbf{Q}\,\mathrm{sgn}(\mathbf{s}) \tag{11}$$

$$\dot{\mathbf{s}} = -\mathbf{PQ}\,\mathrm{sgn}(\mathbf{s}) + (\mathbf{P} - \mathbf{I})\mathbf{\Lambda}(\dot{\mathbf{\Theta}}_d - F(\mathbf{\Theta})) + \mathbf{\Lambda}\tilde{F}(\mathbf{\Theta}) \tag{12}$$

where $\mathbf{P} := \mathbf{\Lambda}(G + \tilde{G})(\mathbf{\Lambda} G)^{-1}$, which is very close to the identity matrix, and $\mathbf{Q}$ is a positive-definite diagonal matrix chosen by the designer. If one sets $\mathbf{T} := \boldsymbol{\tau}_{\mathbf{SMC}}$, then the system enters the sliding mode after a reaching phase.

The expression in (12) can be interpreted as follows:

- If there are no uncertainties, i.e. $\tilde{F} = \mathbf{0}$ and $\tilde{G} = \mathbf{0}$, then we have $\dot{\mathbf{s}} = -\mathbf{Q}\,\mathrm{sgn}(\mathbf{s})$, and $\mathbf{s}^{\mathrm{T}}\dot{\mathbf{s}} < 0$ is satisfied with any positive-definite $\mathbf{Q}$. In this case we have $\mathbf{P} = \mathbf{I}$ and this result is straightforward.
- If only $\tilde{G} = \mathbf{0}$, we obtain $\dot{\mathbf{s}} = -\mathbf{Q}\,\mathrm{sgn}(\mathbf{s}) + \mathbf{\Lambda}\tilde{F}$, and $\mathbf{s}^{\mathrm{T}}\dot{\mathbf{s}} < 0$ is satisfied if $\mathbf{Q}$ is a positive-definite diagonal matrix and the ith entry in the diagonal of $\mathbf{Q}$ is greater than the supremum value of the ith row of $|\mathbf{\Lambda}\tilde{F}|$. This would preserve the sign of $\mathbf{s}$ in the presence of the term $\mathbf{\Lambda}\tilde{F}$ and the numerical computation would require the bounds of the uncertainties. In this case we have $\mathbf{P} = \mathbf{I}$ too.
- In the most general case, where neither of $\tilde{F}$ nor $\tilde{G}$ is zero, the expression in (12) is obtained. In this case, depending on the uncertainties influencing the input gains ($\tilde{G}$), the matrix $\mathbf{P}$ is very close to the identity matrix, and utilizing the uncertainty bounds, the matrix $\mathbf{Q}$ can be chosen such that the sign of $\mathbf{s}$ is preserved and $\mathbf{s}^{\mathrm{T}}\dot{\mathbf{s}} < 0$ is satisfied.

With an appropriate choice of $\mathbf{Q}$, $\mathbf{s}^{\mathrm{T}}\dot{\mathbf{s}} < 0$ can be obtained for $\|\mathbf{s}\| > 0$, and this result indicates that the error vector defined by the difference $\mathbf{\Theta} - \mathbf{\Theta}_d$ is attracted by the subspace characterized by $\mathbf{s} = \mathbf{0}$ and moves toward the origin according to what is prescribed by $\mathbf{s} = \mathbf{0}$. The motion during $\mathbf{s} \neq \mathbf{0}$ is called the reaching mode, whereas the motion when $\mathbf{s} = \mathbf{0}$ is called the sliding mode. During the latter dynamic mode, the closed loop system exhibits certain degrees of robustness against the modeling uncertainties, yet the system is sensitive to noise as the sign of a quantity that is very close to zero determines the control action heavily.

It is straightforward to show that a hitting to $s_i = 0$ occurs and the hitting time ($t_{h,i}$) for the ith subsystem satisfies the inequality $t_{h,i} \leqslant |s_i(0)|/\mathbf{Q}_{ii}$. One can refer to [15–17] for an in-depth discussion on sliding mode control. Our goal will be to obtain the sliding regime by utilizing an ADALINE structure introduced in the following.

4. SLIDING MODE CONTROL THROUGH A FRACTIONAL ORDER ADAPTATION SCHEME

The classical sliding mode control law given in (11) clearly requires $F(\mathbf{\Theta})$ and $G(\mathbf{\Theta})$. In this section, we will focus on an adaptation law that has the same effect on the closed loop system as (11) does.

DOI: 10.1002/acs

Theorem 4.1
Let $\mathbf{p}_i=(\phi_{i,1},\phi_{i,2},\ldots,\phi_{i,r_i+1})^{\mathrm{T}}$ be an adjustable parameter vector and let $\mathbf{u}_i=(e_i,\dot{e}_i,\ldots,e_i^{(r_i-1)},1)^{\mathrm{T}}$ be an input vector. The input output relation of the controller producing τ_i is given by the ADALINE

$$\tau_i=\mathbf{p}_i^{\mathrm{T}}\mathbf{u}_i,\quad i=1,2,\ldots,n \tag{13}$$

Denote the response obtained with $\mathbf{T}_{\mathbf{SMC}}$ as the desired response and let $\tau_{d,i}$ be the control signal resulting in the desired response at the ith subsystem. Let the bound conditions

$$\left|\sum_{k=1}^{\infty}\frac{\Gamma(1+\beta)}{\Gamma(1+k)\Gamma(1-k+\beta)}(\mathbf{p}_i^{(\beta-k)})^{\mathrm{T}}\mathbf{u}_i^{(k)}\right|\leqslant\mathscr{B}_{1,i} \tag{14}$$

$$|\tau_{d,i}^{(\beta)}|\leqslant\mathscr{B}_{2,i} \tag{15}$$

hold true $\forall i\in\{1,2,\ldots,n\}$. With arbitrary $\mu>0$ and $\rho>0$, the tuning law given by

$$\mathbf{p}_i^{(\beta)}=-\mathscr{K}_i\frac{\operatorname{sgn}(\mathbf{u}_i)}{\mu+\rho\mathbf{u}_i^{\mathrm{T}}\mathbf{u}_i}\operatorname{sgn}(\sigma_i) \tag{16}$$

with $\sigma_i:=\tau_i-\tau_{d,i}$ drives the parameters of the ith controller to values such that the plant under control enters the sliding mode characterized by $s_i=0$, and hitting in finite time occurs if

$$\mathscr{K}_i>(\mu+\rho)(\mathscr{B}_{1,i}+\mathscr{B}_{2,i}) \tag{17}$$

is satisfied.

Proof
Define $\Upsilon_i:=\sum_{k=1}^{\infty}(\Gamma(1+\beta)/\Gamma(1+k)\Gamma(1-k+\beta))(\mathbf{p}_i^{(\beta-k)})^{\mathrm{T}}\mathbf{u}_i^{(k)}$ and check whether the quantity $\sigma_i^{(\beta)}\sigma_i$ for every i is negative or not. With these expressions, we have

$$\begin{aligned}
\sigma_i^{(\beta)}\sigma_i&=(\tau_i^{(\beta)}-\tau_{d,i}^{(\beta)})\sigma_i\\
&=((\mathbf{p}_i^{(\beta)})^{\mathrm{T}}\mathbf{u}_i)\sigma_i+(\Upsilon_i-\tau_{d,i}^{(\beta)})\sigma_i\\
&=\left(\left(-\mathscr{K}_i\frac{\operatorname{sgn}(\mathbf{u}_i)}{\mu+\rho\mathbf{u}_i^{\mathrm{T}}\mathbf{u}_i}\operatorname{sgn}(\sigma_i)\right)^{\mathrm{T}}\mathbf{u}_i\right)\sigma_i+(\Upsilon_i-\tau_{d,i}^{(\beta)})\sigma_i\\
&=-\mathscr{K}_i\frac{\operatorname{sgn}(\mathbf{u}_i)^{\mathrm{T}}\mathbf{u}_i}{\mu+\rho\mathbf{u}_i^{\mathrm{T}}\mathbf{u}_i}|\sigma_i|+(\Upsilon_i-\tau_{d,i}^{(\beta)})\sigma_i\\
&=-\mathscr{K}_i\mathscr{P}(\mathbf{u}_i)|\sigma_i|+(\Upsilon_i-\tau_{d,i}^{(\beta)})\sigma_i\\
&\leqslant-\mathscr{K}_i\mathscr{P}(\mathbf{u}_i)|\sigma_i|+|\Upsilon_i|\ |\sigma_i|+|\tau_{d,i}^{(\beta)}|\ |\sigma_i|\\
&\leqslant(-\mathscr{K}_i\mathscr{P}(\mathbf{u}_i)+\mathscr{B}_{1,i}+\mathscr{B}_{2,i})|\sigma_i|\\
&\leqslant 0\quad\text{since }\mathscr{K}_i>(\mu+\rho)(\mathscr{B}_{1,i}+\mathscr{B}_{2,i})>\frac{\mathscr{B}_{1,i}+\mathscr{B}_{2,i}}{\mathscr{P}(\mathbf{u}_i)}
\end{aligned} \tag{18}$$

where $\mathscr{P}(\mathbf{u}_i):=\operatorname{sgn}(\mathbf{u}_i)^{\mathrm{T}}\mathbf{u}_i/(\mu+\rho\mathbf{u}_i^{\mathrm{T}}\mathbf{u}_i)>0$ and $\min\mathscr{P}(\mathbf{u}_i)=1/(\mu+\rho)$.

DOI: 10.1002/acs

This proves that the trajectories in the phase space are attracted by the subspace described by $\sigma_i = 0$. Owing to the definition in (1), claiming $\sigma_i^{(\beta)}\sigma_i < 0$ for stability is equivalent to the following:

$$\sigma_i^{(\beta)}(t)\sigma_i(t) = \frac{\sigma_i(t)}{\Gamma(1-\beta)}\frac{\mathrm{d}}{\mathrm{d}t}\int_0^t \frac{\sigma_i(\xi)}{(t-\xi)^\beta}\,\mathrm{d}\xi \tag{19}$$

Obtaining $\sigma_i^{(\beta)}(t)\sigma_i(t) < 0$ can arise in the following cases. In the first case, $\sigma_i(t) > 0$ and the integral $\int_0^t (\sigma_i(\xi)/(t-\xi)^\beta)\,\mathrm{d}\xi$ is monotonically decreasing. In the second case $\sigma_i(t) < 0$ and the integral $\int_0^t (\sigma_i(\xi)/(t-\xi)^\beta)\,\mathrm{d}\xi$ is monotonically increasing. In both cases, the signal $|\sigma_i(t)|$ is forced to converge to the origin faster than $t^{-\beta}$. A natural consequence of this is to observe a very fast reaching phase as the signal $t^{-\beta}$ is a very steep function around $t \approx 0$.

Now we must prove that first hitting to the switching function occurs in finite time denoted by $t_{h,i}$. Evaluate $\sigma_i^{(\beta)}$ utilizing (16) as given below:

$$\sigma_i^{(\beta)} = -\mathscr{K}_i \frac{\mathrm{sgn}(\mathbf{u}_i)^{\mathrm{T}}\mathbf{u}_i}{\mu + \rho\mathbf{u}_i^{\mathrm{T}}\mathbf{u}_i}\,\mathrm{sgn}(\sigma_i) + \Upsilon_i - \tau_{d,i}^{(\beta)} \tag{20}$$

Applying the fractional integration operator described in (3) with final time $t = t_{h,i}$ to both sides of (20) one gets

$$\begin{aligned}
\sigma_i(t_{h,i}) - \sigma_i^{(\beta-1)}(0)\frac{t_{h,i}^{\beta-1}}{\Gamma(\beta)} &= {}_0\mathbf{I}_{t_{h,i}}^{\beta}\left(-\mathscr{K}_i \frac{\mathrm{sgn}(\mathbf{u}_i)^{\mathrm{T}}\mathbf{u}_i}{\mu + \rho\mathbf{u}_i^{\mathrm{T}}\mathbf{u}_i}\,\mathrm{sgn}(\sigma_i)\right) + {}_0\mathbf{I}_{t_{h,i}}^{\beta}(\Upsilon_i - \tau_{d,i}^{(\beta)}) \\
&= -\mathscr{K}_i\,\mathrm{sgn}(\sigma_i(0)){}_0\mathbf{I}_{t_{h,i}}^{\beta}\left(\frac{\mathrm{sgn}(\mathbf{u}_i)^{\mathrm{T}}\mathbf{u}_i}{\mu + \rho\mathbf{u}_i^{\mathrm{T}}\mathbf{u}_i}\right) + {}_0\mathbf{I}_{t_{h,i}}^{\beta}(\Upsilon_i - \tau_{d,i}^{(\beta)}) \\
&= -\mathscr{K}_i\,\mathrm{sgn}(\sigma_i(0)){}_0\mathbf{I}_{t_{h,i}}^{\beta}\mathscr{P}(\mathbf{u}_i) + {}_0\mathbf{I}_{t_{h,i}}^{\beta}(\Upsilon_i - \tau_{d,i}^{(\beta)})
\end{aligned} \tag{21}$$

where $\mathscr{P}(\mathbf{u}_i) := \mathrm{sgn}(\mathbf{u}_i)^{\mathrm{T}}\mathbf{u}_i/(\mu + \rho\mathbf{u}_i^{\mathrm{T}}\mathbf{u}_i)$. Noting that $\sigma_i(t) = 0$ when $t = t_{h,i}$, multiplying both sides of (21) by $\mathrm{sgn}(\sigma_i(0))$, we have

$$-\sigma_i^{(\beta-1)}(0)\,\mathrm{sgn}(\sigma_i(0))\frac{t_{h,i}^{\beta-1}}{\Gamma(\beta)} = -\mathscr{K}_i {}_0\mathbf{I}_{t_{h,i}}^{\beta}\mathscr{P}(\mathbf{u}_i) + {}_0\mathbf{I}_{t_{h,i}}^{\beta}(\mathrm{sgn}(\sigma_i(0))\Upsilon_i) - {}_0\mathbf{I}_{t_{h,i}}^{\beta}(\mathrm{sgn}(\sigma_i(0))\tau_{d,i}^{(\beta)}) \tag{22}$$

Owing to the definition given in (3), we have

$$\begin{aligned}
{}_0\mathbf{I}_{t_{h,i}}^{\beta}(\mathrm{sgn}(\sigma_i(0))\Upsilon_i) &\leqslant {}_0\mathbf{I}_{t_{h,i}}^{\beta}|\Upsilon_i| \\
&\leqslant {}_0\mathbf{I}_{t_{h,i}}^{\beta}\mathscr{B}_{1,i} \\
&= \mathscr{B}_{1,i}\frac{t_{h,i}^{\beta}}{\Gamma(1+\beta)}
\end{aligned} \tag{23}$$

DOI: 10.1002/acs

Similarly,

$$
\begin{aligned}
{}_0\mathbf{I}^{\beta}_{t_{h,i}}(\operatorname{sgn}(\sigma_i(0))\tau^{(\beta)}_{d,i}) &= \operatorname{sgn}(\sigma_i(0)){}_0\mathbf{I}^{\beta}_{t_{h,i}}\tau^{(\beta)}_{d,i} \\
&= \operatorname{sgn}(\sigma_i(0))\left(\tau_{d,i}(t_{h,i}) - \tau^{(\beta-1)}_{d,i}(0)\frac{t^{\beta-1}_{h,i}}{\Gamma(\beta)}\right) \qquad (24)
\end{aligned}
$$

Since $\min \mathscr{P}(\mathbf{u}_i) = 1/(\mu+\rho)$, we proceed as follows:

$$
\begin{aligned}
{}_0\mathbf{I}^{\beta}_{t_{h,i}}\mathscr{P}(\mathbf{u}_i) &\leqslant {}_0\mathbf{I}^{\beta}_{t_{h,i}}\frac{1}{\mu+\rho} \\
&= \frac{t^{\beta}_{h,i}}{(\mu+\rho)\Gamma(1+\beta)} \qquad (25)
\end{aligned}
$$

Substituting the results in (23)–(25) into (22), we obtain an inequality given as

$$
\begin{aligned}
-\sigma^{(\beta-1)}_i(0)\operatorname{sgn}(\sigma_i(0))\frac{t^{\beta-1}_{h,i}}{\Gamma(\beta)} &\leqslant -\frac{\mathscr{K}_i t^{\beta}_{h,i}}{(\mu+\rho)\Gamma(1+\beta)} + \mathscr{B}_{1,i}\frac{t^{\beta}_{h,i}}{\Gamma(1+\beta)} - \operatorname{sgn}(\sigma_i(0))\tau_{d,i}(t_{h,i}) \\
&\quad + \tau^{(\beta-1)}_{d,i}(0)\operatorname{sgn}(\sigma_i(0))\frac{t^{\beta-1}_{h,i}}{\Gamma(\beta)} \qquad (26)
\end{aligned}
$$

The inequality above can be rearranged as

$$
\begin{aligned}
\frac{(\mathscr{K}_i - \mathscr{B}_{1,i}(\mu+\rho))}{(\mu+\rho)\Gamma(1+\beta)}t^{\beta}_{h,i} &\leqslant \frac{(\sigma^{(\beta-1)}_i(0) + \tau^{(\beta-1)}_{d,i}(0))\operatorname{sgn}(\sigma_i(0))}{\Gamma(\beta)}t^{\beta-1}_{h,i} - \operatorname{sgn}(\sigma_i(0))\tau_{d,i}(t_{h,i}) \\
&\leqslant \frac{|\sigma^{(\beta-1)}_i(0)| + |\tau^{(\beta-1)}_{d,i}(0)|}{\Gamma(\beta)}t^{\beta-1}_{h,i} + |\tau_{d,i}(t_{h,i})| \qquad (27)
\end{aligned}
$$

which has the form

$$
at^{\beta}_{h,i} \leqslant bt^{\beta-1}_{h,i} + c \qquad (28)
$$

where a, b and c are clear from (27). Clearly, the left-hand side of (28) starts from zero and increases monotonically as $a>0$ and $0<\beta<1$. The right-hand side, however, is monotonically decreasing as $b>0$ and $0<\beta<1$. The curve described on the right starts from infinity when $t_{h,i}=0$ and converges to c in the limit. Therefore, the inequality in (28) always suggests an upper bound.

As a special case, if $\beta=\frac{1}{2}$, the value of $t_{h,i}$ can be computed as given by

$$
t_{h,i} \leqslant \left(\frac{c+\sqrt{c^2+4ab}}{2a}\right)^2 \qquad (29)
$$

□

Remark

The tuning law in (16) can be interpreted as a filtering of the signal $\mathbf{r}_i := -\mathscr{K}_i(\operatorname{sgn}(\mathbf{u}_i)/(\mu+\rho\mathbf{u}_i^{\mathrm{T}}\mathbf{u}_i))$ $\operatorname{sgn}(\sigma_i)$. The filter is a fractional integrator of order β having a higher magnitude than integer order

DOI: 10.1002/acs

integrator at all frequencies except zero. In the integer order case, the information contained in the high frequencies is not exploited as much efficiently as in the fractional order case. The presence of sign term in $\mathbf{r}_i$ is one evidence of the presence of valuable information in high frequencies. The special treatment provided by the fractional order tuning law therefore extracts a better path toward good parameter values than the integer order counterpart.

5. CONDITIONS FOR OBTAINING $\mathrm{sgn}(\sigma)$

In the third section, we summarized the conventional sliding mode control scheme for multi-input multi-output systems of the form (6). On the other hand, if we could know a supervisory signal to compute σ, we would use it directly in the fractional adaptation scheme given in (16). However, the nature of the control systems does not provide such an information; instead, one has to develop strategies to observe a desired response in the closed loop by utilizing available quantities. Therefore, a critically important stage of the approach presented in this paper is to extract an equivalent measure about the sign of the error on the control signal to use in the parameter tuning scheme. In other words, we need to develop a strategy together with a set of assumptions such that we do not implement a conventional sliding mode controller, yet our tuning scheme drives the closed loop system toward the behavior that can be obtained via the conventional design without knowing the system parameters.

For this purpose, denote the response of the ADALINE controllers by $\mathbf{T_A}$, which is $n \times 1$. Since there are n subsystems, there are n ADALINE controllers. Consider the difference

$$\begin{aligned}\boldsymbol{\sigma} &= \mathbf{T_A} - \mathbf{T_{SMC}} \\ &= \mathbf{T_A} + (\boldsymbol{\Lambda}\mathbf{G}(\boldsymbol{\Theta}))^{-1}\boldsymbol{\Lambda}(\mathbf{F}(\boldsymbol{\Theta}) - \dot{\boldsymbol{\Theta}}_d) + (\boldsymbol{\Lambda}\mathbf{G}(\boldsymbol{\Theta}))^{-1}\mathbf{Q}\,\mathrm{sgn}(\mathbf{s}) \\ &= \mathbf{J}\,\mathrm{sgn}(\mathbf{s}) + \mathbf{H} \end{aligned} \tag{30}$$

where $\mathbf{J} := (\boldsymbol{\Lambda}\mathbf{G}(\boldsymbol{\Theta}))^{-1}\mathbf{Q}$ and $\mathbf{H} := \mathbf{T_A} + (\boldsymbol{\Lambda}\mathbf{G}(\boldsymbol{\Theta}))^{-1}\boldsymbol{\Lambda}(\mathbf{F}(\boldsymbol{\Theta}) - \dot{\boldsymbol{\Theta}}_d)$. Let $\mathbf{J}'$ be a diagonal matrix where $\mathbf{J}'_{ii} = \mathbf{J}_{ii}$. Let $\mathbf{H}' := \mathbf{H} + (\mathbf{J} - \mathbf{J}')\ \mathrm{sgn}(\mathbf{s})$. With these definitions, (30) can be paraphrased as

$$\boldsymbol{\sigma} = \mathbf{J}'\,\mathrm{sgn}(\mathbf{s}) + \mathbf{H}' \tag{31}$$

whose rows can explicitly be written as

$$\sigma_i = \mathbf{J}'_{ii}\mathrm{sgn}(s_i) + \mathbf{H}'_i, \quad i = 1, 2, \ldots, n \tag{32}$$

The expression in (32) stipulates that if $|\mathbf{H}'_i| < \mathbf{J}'_{ii}$ then $\mathrm{sgn}(\sigma_i) = \mathrm{sgn}(s_i)$. In other words, aside from the bound conditions given in (14) and (15), a third one is given as follows:

$$0 \leqslant |\mathbf{H}'_i| < \mathbf{J}'_{ii}, \quad i = 1, 2, \ldots, n \tag{33}$$

Note that one can obtain infinitely many different designs of $\mathbf{H}$ including those satisfying the set of inequalities above. Aside from the components coming from the system dynamics and the desired response, this depends also upon $\boldsymbol{\Lambda}$ and $\mathbf{Q}$, the choice of which can change the desired properties of the sliding mode. Therefore one needs to check whether $\mathbf{J}'_{ii}$ is positive or not.

Corollary

If the inequalities in (14) and (15) are satisfied, the tuning law in (16) enforces reaching $\sigma_i = 0$ for $\forall i$ and this triggers the emergence of the sliding mode in the traditional sense. However, the

DOI: 10.1002/acs

conditions derived in this section imply a class of plants where such an induction could be valid. In the following section, we give the dynamical description of a two DOF robot.

6. DYNAMICS OF THE ROBOT ARM AND THE CONTROL PROBLEM

In this paper, we consider the following system to visualize the contributions of this paper. The motivation for choosing this system is the nonlinear and coupled nature of differential equations describing the behavior. Furthermore, the adverse effects of noise, large initial conditions and varying payload conditions make the control problem a challenge for conventional approaches.

The dynamics of the robot is given by

$$\mathbf{M}(\mathbf{\Theta})\ddot{\mathbf{\Theta}}+\mathbf{C}(\mathbf{\Theta},\dot{\mathbf{\Theta}})=\mathbf{T}-\mathbf{L} \tag{34}$$

where $\mathbf{\Theta}=(\theta_1\ \ \theta_2)^{\mathrm{T}}$ is the vector of angular positions in radians and $\dot{\mathbf{\Theta}}=(\dot{\theta}_1\ \ \dot{\theta}_2)^{\mathrm{T}}$ is the vector of angular velocities in rad/s. In (34), $\mathbf{T}=(\tau_1\ \ \tau_2)^{\mathrm{T}}$ is the vector of control inputs (torques) and $\mathbf{L}=(\eta_1\ \ \eta_2)^{\mathrm{T}}$ is the vector of friction forces. The terms in (34) are given below:

$$\mathbf{M}(\mathbf{\Theta})=\begin{pmatrix} p_1+2p_3\cos(\theta_2) & p_2+p_3\cos(\theta_2) \\ p_2+p_3\cos(\theta_2) & p_2 \end{pmatrix} \tag{35}$$

$$\mathbf{C}(\mathbf{\Theta},\dot{\mathbf{\Theta}})=\begin{pmatrix} -\dot{\theta}_2(2\dot{\theta}_1+\dot{\theta}_2)p_3\sin\theta_2 \\ \dot{\theta}_1^2 p_3\sin\theta_2 \end{pmatrix} \tag{36}$$

where $p_1=3.31655+0.18648M_p$, $p_2=0.1168+0.0576M_p$ and $p_3=0.16295+0.08616M_p$. Here, M_p denotes the payload mass. The details of the plant model can be found in [18, 19]. The constraints regarding the plant dynamics are $|\tau_1|\leqslant 245\,\mathrm{N}$, $|\tau_2|\leqslant 39.2\,\mathrm{N}$, and the friction terms are $\eta_1=4.9\,\mathrm{sgn}(\dot{\theta}_1)$ and $\eta_2=1.67\,\mathrm{sgn}(\dot{\theta}_2)$.

The control problem is to force the system states to a predefined and differentiable trajectories within the workspace of the robot. More explicitly, $e_1=\theta_1-\theta_{d,1}$, $e_2=\theta_2-\theta_{d,2}$ and the first order (integer) time derivatives of these error terms are desired to converge to the origin of the phase space.

According to the presented analysis and the model above, we have $(\mathbf{\Lambda G})^{-1}=\mathbf{M}(\mathbf{\Theta})$. More explicitly,

$$(\mathbf{\Lambda G})^{-1}\mathbf{Q}=\begin{pmatrix} \mathbf{Q}_{11}(p_1+2p_3\cos(\theta_2))\,\mathrm{sgn}(s_1) \\ \mathbf{Q}_{22}p_3\,\mathrm{sgn}(s_2) \end{pmatrix}+\begin{pmatrix} \mathbf{Q}_{22}(p_1+p_3\cos(\theta_2))\,\mathrm{sgn}(s_2) \\ \mathbf{Q}_{11}(p_1+p_3\cos(\theta_2))\,\mathrm{sgn}(s_1) \end{pmatrix} \tag{37}$$

The above separation of terms suggests that $\mathbf{J}'_{11}=\mathbf{Q}_{11}(p_1+2p_3\cos(\theta_2))>0$ and $\mathbf{J}'_{22}=\mathbf{Q}_{22}p_3>0$ for every possible angular state and payload condition. Clearly, the devised approach is suitable for mechanical systems, robots and systems as they have a positive-definite inertia matrix. In the

DOI: 10.1002/acs

following section, we present the simulation studies comparatively with the integer order integration scheme in the parameter adaptation stage.

7. SIMULATION RESULTS

The presented approach is implemented for the plant introduced in the second section. We set $\beta=\frac{1}{2}$ and the system runs for 20 s of time for the reference trajectories shown in Figure 1. The solid curves represent the reference trajectories, while the dashed ones stand for the response of the robot. During the operation, a 5 kg of payload is grasped when $t=4$ s and released when $t=8$ s and this is repeated when the robot is motionless at $t=12$ and 16 s. The manipulator is desired to stay motionless after $t=16$ s.

It should be noted that the payload scenario is a significant disturbance changing the dynamics of the plant suddenly. Another difficulty is the initial conditions that the ADALINE controllers are supposed to alleviate. Initially, $\theta_{d,1}=\theta_{d,2}=0$, the system is motionless and $\theta_1(0)=\frac{\pi}{3}$ and $\theta_2(0)=-\frac{\pi}{2}$, which indicate large initial positional errors to test the performance of the proposed control scheme. During the simulations, we set $\mathscr{K}_1=500$ and $\mathscr{K}_2=100$. The sliding lines for both links are set by choosing $\lambda_i=1$ and we set $\mu=1$ and $\rho=1$. Besides these, in order to avoid exciting any undesired chattering phenomenon associated tightly with the discontinuous nature of

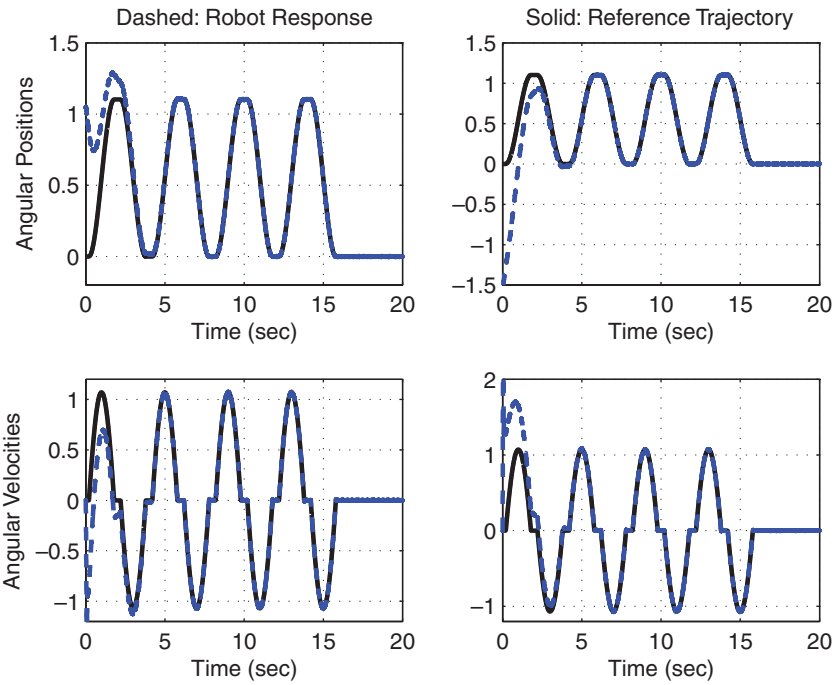

Figure 1. Reference trajectories and the response of the robot.

DOI: 10.1002/acs

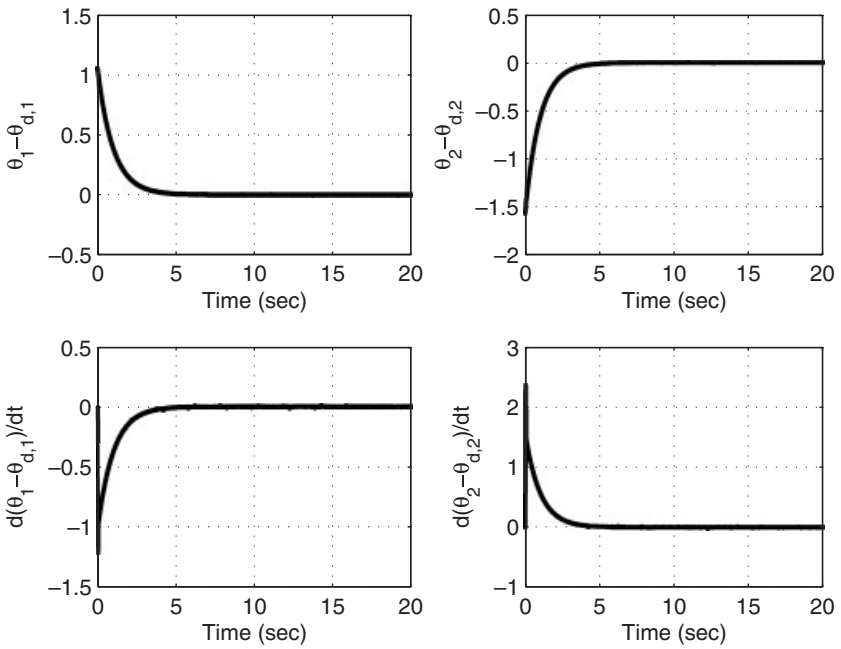

Figure 2. State tracking errors.

the sign function, we choose $\text{sgn}(\sigma_i) \approx \sigma_i/(|\sigma_i|+\delta)$ with δ being the parameter determining the slope around the origin. This paper considers $\delta = 0.01$, which introduces a very thin boundary layer and improves the performance of the control system. If such a smoothing is not used, the fluctuations in the control signals are magnified and the practical applicability of the proposed approach is influenced adversely.

The discrepancies between the reference trajectories and the system response are depicted in Figure 2, where an exponential convergence is apparent even in the presence of noise corrupting the observed system states and the changes in the system dynamics due to the payload variations.

The behavior in the phase space illustrated in Figure 3 is another evidence of robustness of the control system and insensitivity to variations in the plant dynamics. As mentioned previously, a very fast reaching phase is followed by the desired sliding mode.

In Figure 4, the applied control signals are given with the window graphs for better visualizing the initial transient. As expected, the control efforts during the first 0.2 s have higher magnitudes than what comes later. The adverse effect of the noisy observations on the control signal is another conclusion that is worth mentioning.

The time evolutions of the controller parameters, which are all started from zero, are shown in Figure 5, where it is clearly visible that after a fast transient, the parameters multiplying the errors and their derivatives settle down to constant values, while the parameters multiplied by unity evolve bounded. If we remember the reference profiles, the system is desired to be motionless after $t > 16$ s; this means that the tuning activity during this time is subject to the effects of noise. That is to say, the system is at a desired state but we would like to figure out how the parameter

DOI: 10.1002/acs

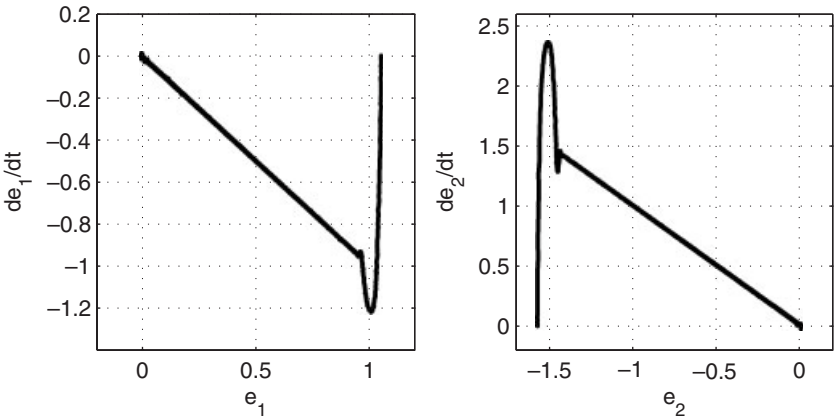

Figure 3. Behavior in the phase space.

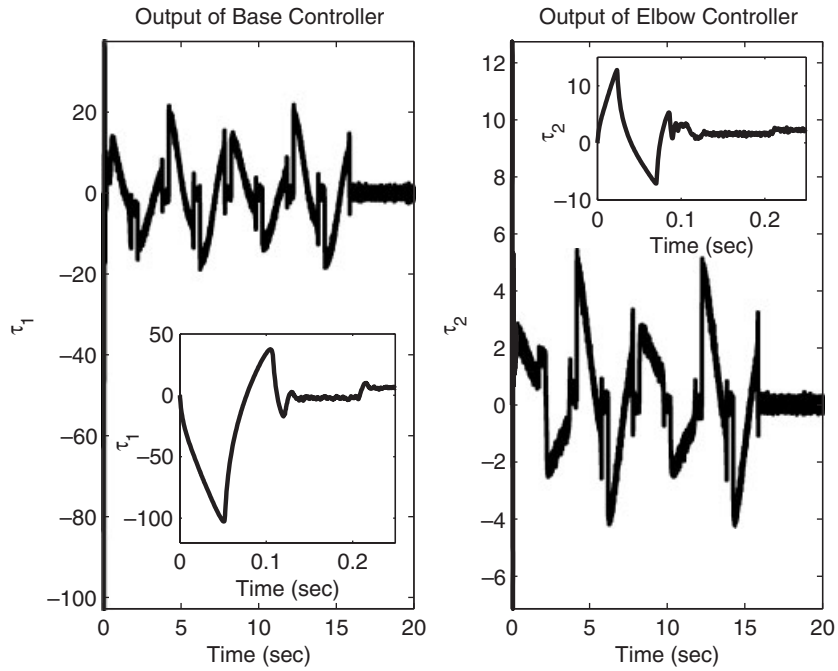

Figure 4. Applied control signals and their initial transients.

tuning mechanism functions during this period. The answer to this question is in Figure 5, where any possible undesired drifts in the controller parameters are suppressed appropriately.

In realizing the tuning law in (16), which entails the implementation of $\mathbf{I}^{0.5}$ terms, we choose Crone approximation over the bandwidth 0.01–1000 Hz, which is acceptable for a feedback

DOI: 10.1002/acs

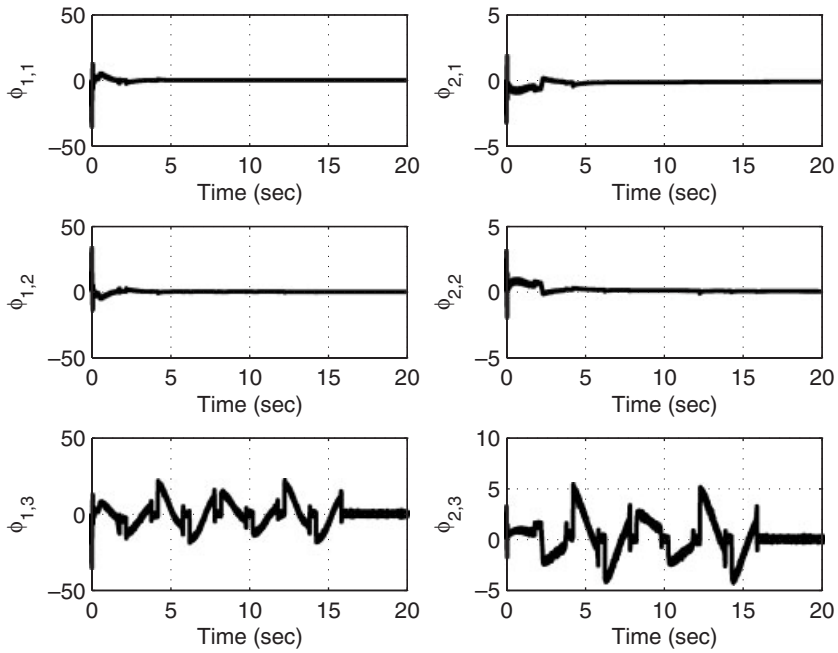

Figure 5. Time evolution of the controller parameters for base link (left column) and elbow link (right column).

control application of this type. The order is set to 25 and truncated Mclaurin expansion is utilized in numerical computation. With these settings, a very good spectral approximation to the desired operator is obtained. For more details on the numerical realization, the reader is referred to [20].

It must be emphasized that the presented design does not utilize the terms seen in the dynamical description of the plant. The approach adaptively determines the controller parameters so that the plant displays robustness against disturbances and uncertainties.

The simulations have been repeated with different values of μ and ρ. We did not consider increasing or decreasing or both as this corresponds to change in $\mathscr{K}_i$, instead of this, we kept $\rho=1$ and re-simulated the system with 0.01, 0.1, 10 and 100 as the values of μ. Including the case with $\mu=10$, the system was observed to respond appropriately, yet for the larger values of μ, the sliding mode disappears, further increase causes the loss of tracking capability totally. A similar response is observed with the change in ρ while μ is kept at unity.

As a last issue, we turned back to $\mu=\rho=1$, and the system is run with $\beta=1$. This has changed the parameter update law given in (16) as $\dot{\mathbf{p}}_i=-\mathscr{K}_i(\mathrm{sgn}(\mathbf{u}_i)/(\mu+\rho\mathbf{u}_i^{\mathrm{T}}\mathbf{u}_i))\,\mathrm{sgn}(\sigma_i)$. We have $\Upsilon_i:=\mathbf{p}^{\mathrm{T}}\dot{\mathbf{u}}_\mathbf{i}$ and the derivation with the conclusions given in (18) is seen valid for the integer order case too. Many different parameter configurations have been tested and, in most of them, the feedback system has grown instabilities. Among the tested conditions, the one with $\mathscr{K}_i=10^5$ has given the best results that are illustrated in Figures 6–9. Although the error trends seen in Figure 6 are promising, the applied torques resulting in this observation are illustrated in Figure 7. Clearly,

DOI: 10.1002/acs

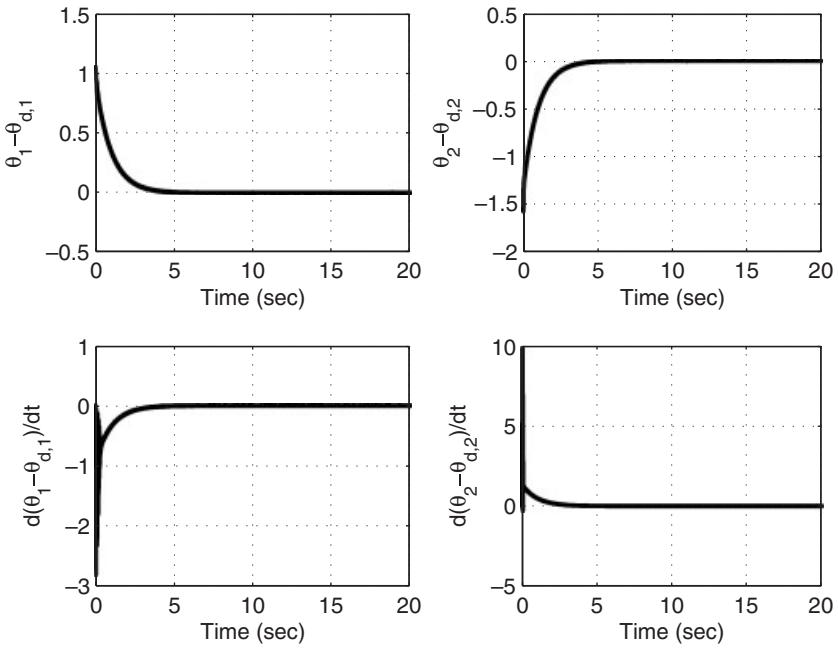

Figure 6. State tracking errors when $\beta = 1$.

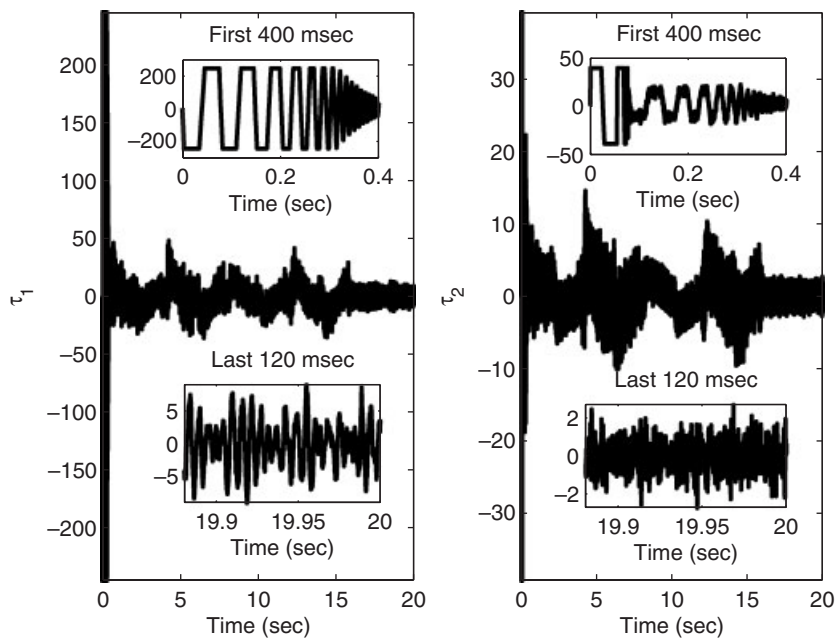

Figure 7. Applied control signals and their initial transients when $\beta = 1$.

DOI: 10.1002/acs

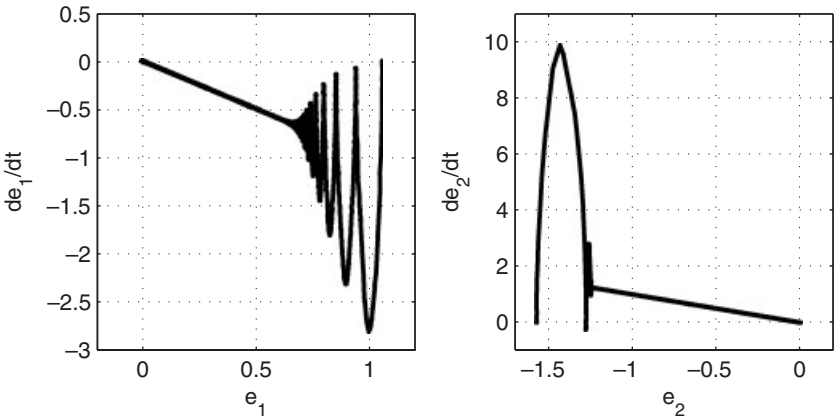

Figure 8. Behavior in the phase space when $\beta = 1$.

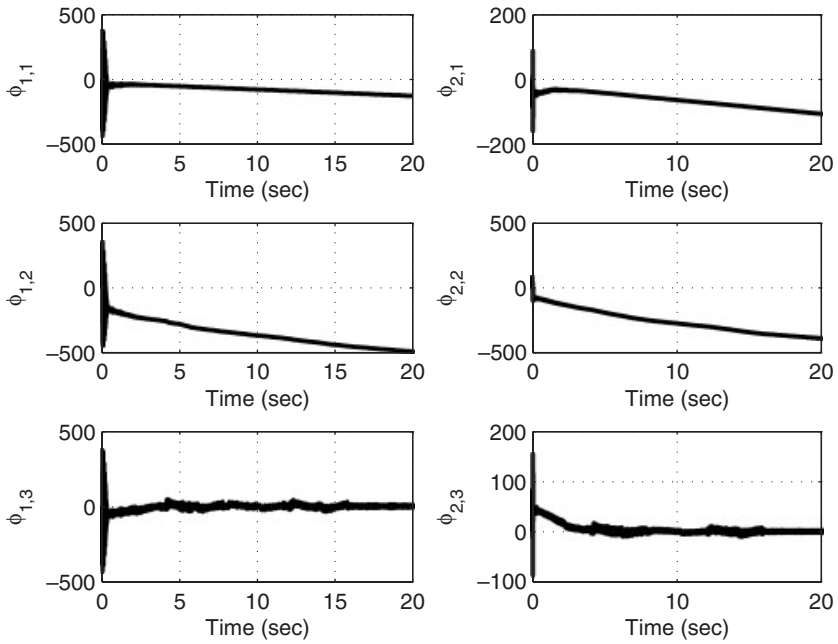

Figure 9. Time evolution of the controller parameters for base link (left column) and elbow link (right column).

the torques have provoked high-frequency components compared with the results of the fractional order case in Figure 4. In addition to this, according to the window plots depicting the initial and final phases of the simulation, the control signals saturate in the early instants of the simulation and are observed to be very sensitive to noise. In Figure 8, the behavior in the phase space is

DOI: 10.1002/acs

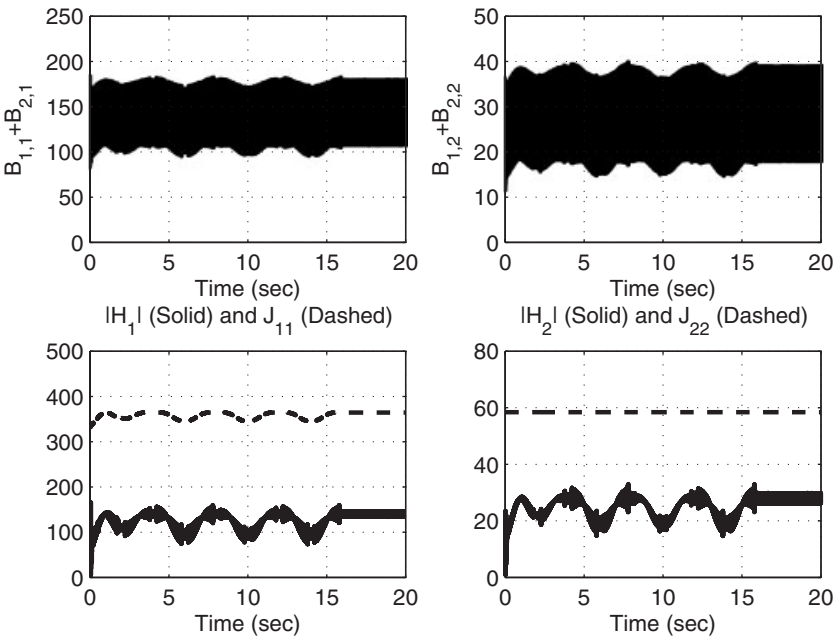

Figure 10. The quantities described in (14), (15) and (33) are satisfied.

depicted for each link separately. Clearly, after many hittings, the sliding regime starts as there are very high controller gains ($\mathcal{K}_i$) and this triggers the saturating control signals whose practical value is arguable.

Despite the fact that the implementation with the integer order case requires costly hardware as its actuation scheme is supposed to produce control signals having demanding spectral qualities, there is another reason making the proposed technique superior than the integer order counterpart: the evolutions of the adjustable parameters. In Figure 9, the behavior of the ADALINE parameters is shown. The first observation is the non-converging nature of the signals, the second is the magnitude plotted in the bottom rows for both controllers, which fluctuates between very high values, indicating a significant potential instability for a real-time application.

Since the figures shown so far support the usefulness of the presented approach, although it is an open problem, we validate the design by checking whether the conditions given in (14), (15) and (33) are satisfied. It is seen from the figure that with the chosen parameters, the prescribed bound conditions are satisfied with the choice $\mathbf{Q}=\begin{pmatrix} 100 & 0 \\ 0 & 500 \end{pmatrix}$ (Figure 10).

Final notes in this section are on the choice $\beta=0.5$. As β approaches unity, the robustness is lost smoothly and many hittings take place before the sliding regime starts; on the other hand, as β approaches zero, the errors signals are deteriorated and the control system becomes extremely vulnerable to noise. This naturally suggests choosing $\beta=0.5$, which is equally distant to the mentioned undesired regimes.

Overall, these results are indications of the usefulness of the proposed technique, which is based on fractional calculus.

DOI: 10.1002/acs

8. CONCLUSIONS

In this paper, we propose a fractional order parameter tuning scheme. The dynamic model of a DOF direct drive robotic manipulator is utilized to justify the claims and a set of trials have been considered for making a comparison with the integer order version. After a comparison with the integer order case, the presented form of the adaptation law provides:

- better parametric evolution that displays no drifts,
- better tracking capabilities,
- better robustness and disturbance rejection capabilities,
- easier initialization of controller parameters,
- less sensitivity to measurement noise

than its integer order counterpart, which is only computationally simple.

Briefly, according to the considered application, the fractional order tuning law outperforms the tuning mechanisms exploiting integer order operators.

Although seen empirically in this example, future work of the author aims to provide a rigorous proof for the bounded evolution of the adjustable parameters.

ACKNOWLEDGEMENTS

The Matlab toolbox *Ninteger v.2.3*[¶] is used and the efforts of its developer, Dr Duarte Valério, are gratefully acknowledged. This work is supported by Turkish Scientific Council (TÜBİTAK) Contract 107E137.

REFERENCES

1. Haykin S. *Neural Networks*. Macmillan College Printing Company: New Jersey, 1994.
2. Jang J-SR, Sun C-T, Mizutani E. *Neuro-fuzzy and Soft Computing*. PTR Prentice-Hall: Upper Saddle River, NJ, U.S.A., 1997.
3. Oldham KB, Spanier J. *The Fractional Calculus*. Academic Press: New York, 1974.
4. Podlubny I. *Fractional Differential Equations* (1st edn). Elsevier Science & Technology Books: San Diego, U.S.A., 1998.
5. Matignon D. Stability properties for generalized fractional differential systems. *ESAIM Proceedings*, Paris, France, vol. 5, 1998; 145–158.
6. Momani S, Hadid S. Lyapunov stability solutions of fractional integrodifferential equations. *International Journal of Mathematics and Mathematical Sciences* 2004; **2004**(47):2503–2507.
7. Åström KJ, Wittenmark B. *Adaptive Control* (2nd edn). Addison-Wesley: Reading, MA, 1995.
8. Vinagre BM, Petraš I, Podlubny I, Chen YQ. Using fractional order adjustment rules and fractional order reference models in model-reference adaptive control. *Nonlinear Dynamics* 2002; **29**:269–279.
9. Ladaci S, Charef A. On fractional adaptive control. *Nonlinear Dynamics* 2006; **43**:365–378.
10. Suárez JI, Vinagre BM, Chen YQ. A fractional adaptation scheme for lateral control of an AGV. *2nd IFAC Workshop on Fractional Differentiation and its Applications*, Porto, Portugal, 19–21 July 2006.
11. Calderón AJ, Vinagre BM, Feliu V. Fractional order control strategies for power electronic buck converters. *Signal Processing* 2006; **88**:2803–2819.
12. Vinagre BM, Calderón AJ. On fractional sliding mode control. *7th Portuguese Conference on Automatic Control* (*CONTROLO'2006*), Lisbon, Portugal, 11–13 September 2006.
13. Yildiz Y, Sabanovic A, Abidi K. Sliding-mode neuro-controller for uncertain systems. *IEEE Transactions on Industrial Electronics* 2007; **54**:1676–1685.

[¶] http://mega.ist.utl.pt/∼dmov/ninteger/ninteger.htm.

DOI: 10.1002/acs

14. Huh S-H, Bien Z. Robust sliding mode control of a robot manipulator based on variable structure-model reference adaptive control approach. *IET Control Theory and Applications* 2007; **1**:1355–1363.
15. Utkin VI. *Sliding Modes in Control Optimization*. Springer: New York, 1992.
16. Edwards C, Spurgeon SK. *Sliding Mode Control Theory and Applications*. Taylor & Francis: London, 1998.
17. Perruquetti W, Barbot JP. *Sliding Mode Control in Engineering*. Marcel Dekker: New York, 2002.
18. *Direct Drive Manipulator R&D Package*, *User Guide*. Integrated Motions Inc., Berkeley, CA, U.S.A., 1992.
19. Efe MÖ, Kaynak O. A comparative study of soft computing methodologies in identification of robotic manipulators. *Robotics and Autonomous Systems* 2000; **30**:221–230.
20. Valério D. *Ninteger v. 2.3 Fractional Control Toolbox for MatLab*, 2005.

DOI: 10.1002/acs